Comprehensive evaluation of the linear stability of Alfvén eigenmodes driven by alpha particles in an ITER baseline scenario

A. C. A. Figueiredo[1], P. Rodrigues[1], D. Borba[1], R. Coelho[1], L. Fazendeiro[1], J. Ferreira[1], N. F. Loureiro[1], F. Nabais[1], S. D. Pinches[2], A. Polevoi[2] and S. E. Sharapov[3]

[1] *Instituto de Plasmas e Fusão Nuclear, Instituto Superior Técnico, Universidade de Lisboa, 1049-001 Lisboa, Portugal*

[2] *ITER Organization, Route de Vinon-sur-Verdon, CS 90 046, 13067 St Paul-lez-Durance Cedex, France*

[3] *CCFE, Culham Science Centre, Abingdon OX14 3DB, United Kingdom*

Introduction

In ITER, the performance of burning plasmas will depend on the population of alpha particles being well confined within the plasma core, as the heating of the DT plasma will then rely mainly on the energy of these suprathermal particles that are produced by core fusion reactions. A phenomenon that can potentially hinder the successful operation of ITER is therefore the destabilization of Alfvén eigenmodes (AEs) by alpha particles [Fu 1989], whereby an increased radial transport of the latter could degrade the conditions necessary to sustain the fusion process and carry damaging heat loads to the tokamak wall [Sharapov 2013]. In this work the stability of AEs is systematically addressed for the 15 MA ELMy H-mode ITER baseline scenario [Polevoi 2002, Pinches 2015, Lauber 2015, Rodrigues 2015] making use of a recently introduced framework [Rodrigues 2015] that is based on the hybrid MHD drift-kinetic code Castor-K [Borba 1999, Nabais 2015].

Results and Discussion

We consider two variants of the aforementioned ITER scenario with plasma current $I_p = 15$ MA, toroidal magnetic field $B_0 = 5.3$ T, and plasma major and minor radii $R_0 = 6.4$ m and $a = 2$ m, respectively[1]. The kinetic profiles in Figure 1 are plotted versus the radial coordinate s, the square root of the poloidal magnetic flux normalized to its boundary value. Both scenario variants have approximately the same electron density n_e and impurity content n_Z, which is essentially Be, and the fuel density $n_{DT} = n_D + n_T$ is for an optimal mix of D and T, i.e., $n_D = n_T$. The main difference between the two variants is that in the one on the left of Figure 1, hereafter called *LoPed*, electron and ion temperatures T_e and T_i, respectively, are much lower at the pedestal and much higher at the core than in the *HiPed* variant on the right. Naturally, the higher core temperatures go with a much higher density of alpha particles n_α and helium ashes (thermalized alpha particles) n_{He} in *LoPed*. For convenience, differences in the safety factor q are discussed apropos Figure 4.

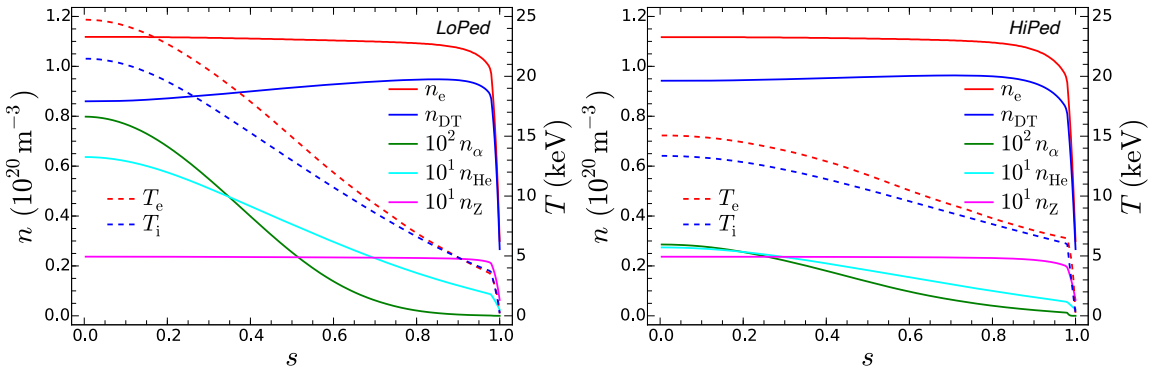

Figure 1. Kinetic profiles for the two variants of the 15 MA ITER baseline scenario. Compared with the *LoPed* scenario, *HiPed* is characterised by higher temperatures at the pedestal and lower core temperatures, together with a lower density of alpha particles and He ashes.

[1] Here, R_0 is the position of the magnetic axis.

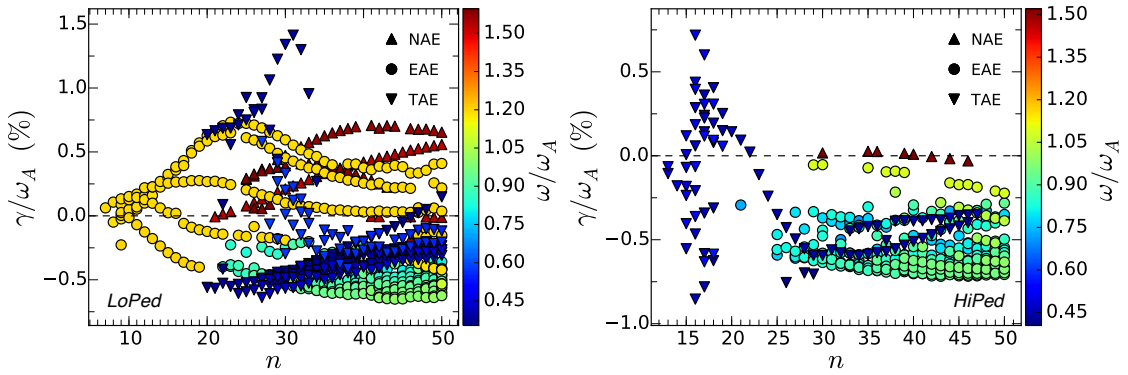

Figure 2. Linear growth rates γ normalized to the Alfvén frequency $\omega_A = v_A/R_0$, where the Alfvén velocity at the magnetic axis is $v_A \approx 7.1\times10^6$ m/s in *LoPed* and $v_A \approx 7.0\times10^6$ m/s in *HiPed*, versus toroidal mode number n and colored by AE frequency for the two variants of the 15 MA ITER baseline scenario. Different symbols are used for Toroidicity induced AEs (TAEs), Ellipticity induced AEs (EAEs), and Non-circular triangularity-induced AEs (NAEs). TAEs appear in dark-blue patterns corresponding to frequencies around $\omega_A/2$ (the middle of the TAE gap) and are the most unstable. No valid AEs have been found for $n < 7$ in *LoPed* and $n < 13$ in *Hiped*.

Besides Castor-K, which assesses the stability of AE by computing their linear growth-rates, our suite of numerical codes comprises Helena [Huysmans 1991] to obtain equilibria and Mishka [Mikhailovskii 1997] to calculate eigenmodes. AEs have been extensively considered in our methodical approach, a necessity that stems from our purpose of forecasting experimental results, rather than interpret them. Here, we focus on values of n ranging from 1 to 50 in order to stay within the limits of the drift-kinetic ordering for the alpha particles [Rodrigues 2015]. All possible AEs have been determined by scanning the mode frequency ω/ω_A from 0.01 to 2 in steps of 2×10^{-5} and inputting $(\omega/\omega_A)^2$ to Mishka as a guess of the eigenvalue that, upon convergence, is returned together with the mode eigenfunction. A selection of valid AEs has then been made based on two criteria: the mode frequency cannot match the Alfvén continuum at any radial position where the mode amplitude is above 1% of its maximum, and the eigenfunction must be well-resolved radially with a numerical grid index $h_g < 0.3$ [Rodrigues 2015]. Around 2300 AEs were selected for *LoPed* and 400 for *HiPed*. These AEs were then processed by Castor-K, which calculates the energy δW_p exchanged between a mode and a given population (P) of plasma particles as well as the associated growth rate $\gamma_P = \mathrm{Im}(\delta W_P)/(2\omega W_k)$, where W_k is the kinetic energy of the mode perturbation [Borba 1999]. For each mode, four Castor-K runs were done to calculate the drive due to the alpha particles

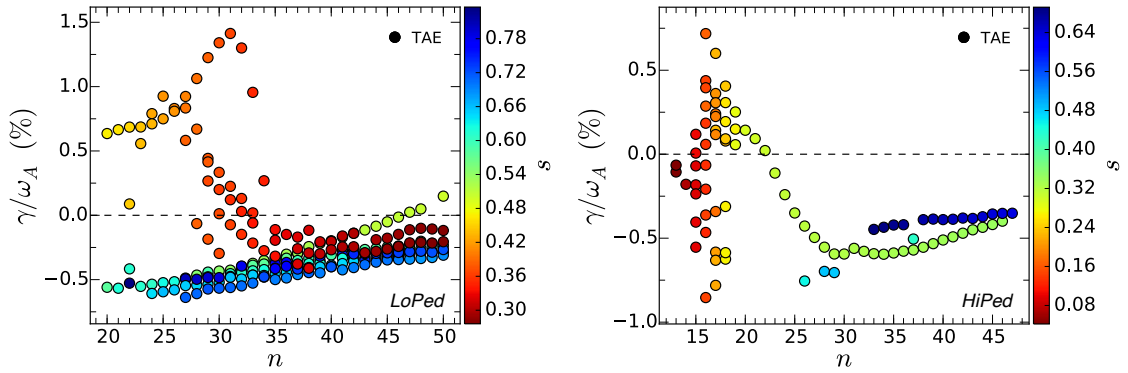

Figure 3. In both analysed scenarios the most unstable TAEs are core-localized. As seen from the q profile in Figure 4, in *HiPed* these TAEs are inside the $q = 1$ surface, so they are 'tornado modes' [Sharapov 2013]. Due to the closing of the TAE gap few modes exist for $n > 20$ in *HiPed* — only those located at the bottom of the gap that avoid matching the continuous spectrum, as seen in Figure 5. Such is not the case in *LoPed* for which more modes exist for high n due to the extended low magnetic-shear region that makes gaps close at an outer position, as seen in Figure 4, and because in *LoPed* higher-n modes are located at inner positions than lower-n modes. Moreover, the higher magnetic shear in *HiPed* does not allow the existence of Low Shear TAEs (LSTAEs) beyond $s \approx 0.3$.

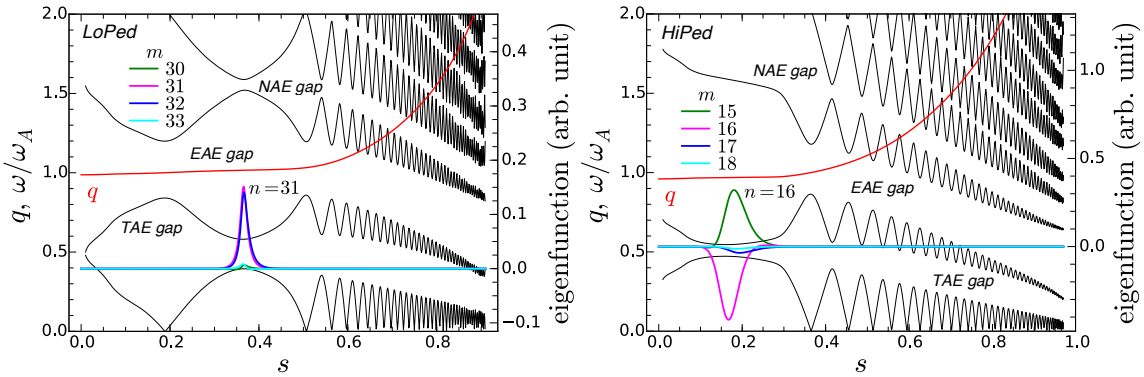

Figure 4. The eigenfunctions of the most unstable AEs represented by the colored lines have been calculated by Mishka using 17 harmonics with poloidal mode number starting at $m = n - 1$, but only the strongest 4 are shown. In both scenario variants the modes fall within the TAE gap of the Alfvén continuous spectrum. Notice that the baseline of the eigenfunction (zero value on the right axis) marks the mode frequency on the left axis. The on-axis value of the safety factor in *HiPed* is $q(0) = 0.96$, around 3% lower than $q(0) = 0.987$ in *LoPed*. While in *HiPed* the low magnetic-shear region ranges from the axis to $s \approx 0.3$, in *LoPed* it extends to $s \approx 0.5$. The $q = 1$ surface is located at $s \approx 0.2$ in *LoPed* and $s \approx 0.37$ in *HiPed*.

(α) and the damping due to the interaction with the bulk ions (DT), the electrons (e), and the helium ashes (He), thus obtaining the total growth rate $\gamma = \gamma_\alpha + \gamma_{DT} + \gamma_e + \gamma_{He}$ of the AE. The alpha-particle population has been described by a radius-independent slowing-down energy distribution with a crossover energy $E_c \approx 730$ keV in *LoPed* and $E_c \approx 585$ keV in *HiPed*, and a dispersion around the alpha-particle birth energy $\Delta_E \approx 50$ keV in both cases [Rodrigues 2015]. Radiative damping, which has a non-negligible contribution to γ in *LoPed* [Rodrigues 2015] will be included in a forthcoming article [Figueiredo 2015].

The growth rates[2] shown in Figures 2 and 3 are larger in *LoPed* than in *HiPed*. Although EAEs and NAEs have positive growth rates in *LoPed*, all markedly unstable modes are TAEs in the vicinity of $n = 30$ in *LoPed* and $n = 15$ in *HiPed*. Figure 3 shows a difference in the evolution of TAE localization as n increases: while in *HiPed* modes become progressively located at outer positions, the opposite occurs in *LoPed*. This results directly from q being below 1 in *HiPed* and above 1 in *LoPed* within the region $0.2 < s < 0.37$. Notice that the unstable modes in Figure 3 are LSTAEs, well-localized and within the low magnetic-shear region of the plasma core. As shown in Figure 4, in *LoPed* the most unstable mode is a $n = 31$ TAE located at $s \approx 0.37$ near the bottom of the TAE gap with a growth rate $\gamma/\omega_A \approx 1.41\%$, whereas in *HiPed* the most unstable mode is a $n = 16$ TAE at $s \approx 0.17$ near the top of the TAE gap with $\gamma/\omega_A \approx 0.72\%$. While in *LoPed* the most unstable mode is close to $s = 0.38$ where the gradient of n_α is highest, that is not possible in *HiPed* because the maximum n_α gradient occurs at $s \approx 0.44$ where the higher magnetic shear only allows non-local modes that interact strongly with the Alfvén continuum. At this point it is interesting to verify the estimate of n for the most driven AE that is based on matching the width of passing alpha-particle orbits and the TAE width [Pinches 2015,

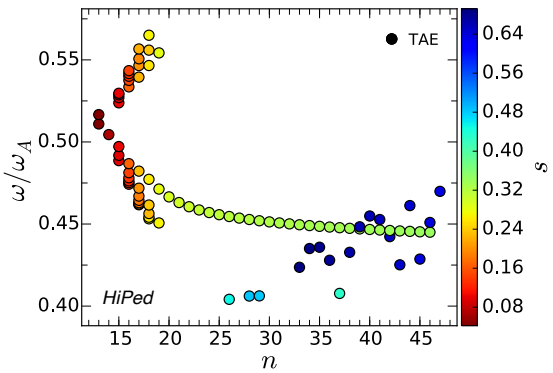

Figure 5. Frequency distribution of "tornado modes" inside the TAE gap in *HiPed*. The lower frequency branch is formed by symmetric modes at the bottom of the gap, while the modes in the upper branch are anti-symmetric TAEs located at the top of the gap.

[2] Notice the normalization to the Alfvén frequency instead of the more usual mode frequency.

Rodrigues 2015], which is given by $n \approx s/q^2 \times a/R_0 \times \Omega_\alpha/\omega_A$. The cyclotron frequency of the alpha particles is $\Omega_\alpha \approx 2.5\times10^8$ rad/s and $q(s)$ is taken at the mode location. Using $q(0.37) \approx 1.016$ we arrive at $n \approx 26$ in *LoPed*, while in *HiPed* $q(0.17) \approx 0.968$ leads to $n \approx 13$.

In Figure 5 the frequency of TAEs is plotted versus n for *HiPed*. Two main branches are evident inside the TAE gap: an upper branch made of modes that rise in frequency as n increases, and a lower branch with decreasing frequency modes. The lower-frequency branch is made of symmetric modes, while the modes in the upper branch are anti-symmetric [Pinches 2015, Lauber 2015]. Moreover, for a given n the number of oscillations in the poloidal harmonics of these modes increases as the frequency increases in the upper branch, or as the frequency decreases in the lower branch. The long line that chirps down until $n \approx 45$ has the simplest symmetric TAEs with a single peak per m (no oscillations). Its 'mirror' line in the upper branch ends abruptly at $n \approx 20$. This occurs because the TAE gap closes at an inner s for modes at the top of the gap than at its bottom, causing the missing modes to be strongly affected by continuum damping.

Summary

The linear-stability of AEs for two variants of the 15 MA ELMy H-mode ITER baseline scenario has been analysed using the hybrid MHD drift-kinetic code Castor-K. The main difference between the two variants *LoPed* and *HiPed* is in the temperature profiles, particularly at the edge pedestal. Results show that the most unstable modes are TAEs with n around 30 in *LoPed* and 15 in *HiPed*. In both variants of the ITER scenario these unstable TAEs are localized in a low magnetic-shear region of the plasma core. In the *HiPed* case a clear frequency distribution of symmetric and anti-symmetric TAEs, which are in fact 'tornado modes', has been found within the TAE gap that agrees with recent studies on the same ITER scenario [Pinches 2015, Lauber 2015]. Calculation of radiative damping is underway and will be part of a following publication. While radiative damping has been shown to somewhat reduce the highest *LoPed* growth rates [Rodrigues 2015], it should not alter our results for *HiPed* significantly since its most unstable mode is an anti-symmetric TAE, which is therefore practically unaffected by radiative damping [Nyqvist 2012].

Acknowledgments

This work has been carried out within the framework of the EUROfusion Consortium and has received funding from the Euratom research and training programme 2014-2018 under grant agreement No. 633053. IST activities received financial support from "Fundação para a Ciência e Tecnologia" (FCT) through project UID/FIS/50010/2013. The views and opinions expressed herein do not necessarily reflect those of the European Commission, IST, FCT, or the ITER Organization. All computations were carried out using the HELIOS supercomputer system at the Computational Simulation Centre of the International Fusion Energy Research Centre (IFERC-CSC) in Aomori, Japan, under the Broader Approach collaboration between Euratom and Japan implemented by Fusion for Energy and JAEA. PR was supported by EUROfusion Consortium grant no. WP14-FRF-IST/Rodrigues and NFL was supported by FCT grant no. IF/00530/2013.

References

[Borba 1999] D. Borba and W. Kerner, J. Comput. Phys. **153** (1999) 101.
[Figueiredo 2015] A. C. A. Figueiredo *et al.* "Comprehensive evaluation of the linear stability of Alfvén eigenmodes driven by alpha particles in an ITER baseline scenario", to be submitted to Nucl. Fusion (2015).
[Fu 1989] G. Y. Fu and J. W. Van Dam, Phys. Fluids B **1** (1989) 1949.
[Huysmans 1991] G. Huysmans *et al.*, Int. J. Mod. Phys. C **2** (1991) 371.
[Lauber 2015] P. Lauber, Plasma Phys. Control. Fusion **57** (2015) 054011.
[Mikhailovskii 1997] A. Mikhailovskii *et al.*, Plasma Phys. Rep. **23** (1997) 844.
[Nabais 2015] F. Nabais *et at.*, Plasma Sci. Technol. **17** (2015) 89.
[Nyqvist 2012] R. M. Nyqvist and S. E. Sharapov, Phys. Plasmas **19** (2012) 082517.
[Pinches 2015] S. D. Pinches *et al.*, Phys. Plasmas **22** (2015) 021807.
[Polevoi 2002] A. R. Polevoi *et al.*, J. Plasma Fusion Res. SERIES **5** (2002) 82.
[Rodrigues 2015] P. Rodrigues *et al.* "Systematic linear-stability assessment of Alfvén eigenmodes in the presence of fusion α-particles for ITER-like equilibria", accepted by Nucl. Fusion (2015).
[Sharapov 2013] S. E. Sharapov *et al.* Nucl. Fusion **53** (2013) 104022.